



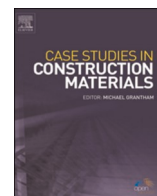
## **Long-term (2 years) drying shrinkage evaluation of alkali-activated slag mortar: Experiments and partial factor analysis**

Downloaded from: <https://research.chalmers.se>, 2025-12-04 19:03 UTC

Citation for the original published paper (version of record):

Wang, S., Wu, K., Yang, Z. et al (2023). Long-term (2 years) drying shrinkage evaluation of alkali-activated slag mortar: Experiments and partial factor analysis. *Case Studies in Construction Materials*, 18.  
<http://dx.doi.org/10.1016/j.cscm.2023.e01956>

N.B. When citing this work, cite the original published paper.



## Case study

# Long-term (2 years) drying shrinkage evaluation of alkali-activated slag mortar: Experiments and partial factor analysis

Shunfeng Wang<sup>a,b</sup>, Kai Wu<sup>a</sup>, Zhenghong Yang<sup>a,\*</sup>, Luping Tang<sup>b,\*</sup>

<sup>a</sup> Key Laboratory of Advanced Civil Engineering Materials of Ministry of Education, School of Materials Science and Engineering, Tongji University, Shanghai 201804, China

<sup>b</sup> Division of Building Technology, Chalmers University of Technology, 41296 Gothenburg, Sweden

## ARTICLE INFO

## Keywords:

Alkali-activated slag mortar

Shrinkage

Compressive strength

Partial factor analysis

## ABSTRACT

Alkali-activated slag with many excellent properties was regarded as a novel low carbon building material, has received more and more attention. This research aims to study the impacts of alkali solution (alkali content and modulus), cement and gypsum contents on compressive strength, weight loss and drying shrinkage for alkali-activated slag mortar. Gypsum used as expanding source could compensate the drying shrinkage caused by silica and alkali components in the first three months, but it has a negative impact on the strength. The mainly results can be concluded that the alkali-activated slag blended with a cement content up to 20 wt% could effectively reduce the shrinkage and weight loss and increase the strength. Furthermore, the alkali content was below 3 wt%, the specimens possess relatively lower drying shrinkage. Based on the results of the test and analysis, the partial factors of combined activation on compressive strength and drying shrinkage of alkali-activated slag mortar were put forward. In the meantime, the relationships between compressive strength and combined activation factor are liner at 28, 90 and 365 days. Compressive strength and drying shrinkage could be estimated according to the combined activation and partial factor analysis. This work could provide a reasonable method for preparing the alkali-activated slag mortar and predict the shrinkage at different periods.

## 1. Introduction

Portland cement as the largest manufactured building materials all over the world was widely used in various housing and infrastructure engineering. A large amount of CO<sub>2</sub> will be released along with the production of cement, which accounts for 6–7% of global anthropogenic emission [1–5]. Considering the energy consumption and CO<sub>2</sub> emissions, it is urgent to develop new type of low-carbon cementitious materials. Alkali-activated materials have attracted more and more attention in the past decades due to reduced costs [6–8], improved mechanical properties and durability [9,10], and less CO<sub>2</sub> emission [11]. Moreover, a variety of industrial by-products (such as fly ash [12], ground granulated blast-furnace slag [13], steel slag [14], red mud [15], etc.) can be recycled as precursors to prepare the alkali-activated materials, which could solve the occupation of land and pollution of environment [16,17]. Among them, alkali-activated slag (AAS) is one of the most extensive studied materials in the past decades, and most of

\* Corresponding authors.

E-mail addresses: [tjzhy92037@163.com](mailto:tjzhy92037@163.com) (Z. Yang), [tang.luping@chalmers.se](mailto:tang.luping@chalmers.se) (L. Tang).

researchers has been regarded as green building materials for Portland cement [18–22].

Although the alkali-activated slag may be alternative to Portland clinker based cements, the volume instability highly limited its application in the large-scale civil engineering. In order to extent the application of alkali-activated slag in the construction sites, the volume stability must be strictly controlled. In the meantime, the large shrinkage for AAS is due to the fine pore structure [23–25] and its gel characteristic of hydration products [2,26]. Most of studies concentrated on the impacts of raw materials [10,27], curing regime [28,29] and the type and dosage of alkali activator [18,30–32] on the shrinkage of alkali-activated slag. The drying shrinkage of AAS would gradually increase with the increase of alkali content. The high content of alkali not only promotes the reaction, but also increases the capillary pressure in the hardened alkali-activated slag paste [2,28,32,33]. The effect of alkali activators type (NaOH, Na<sub>2</sub>CO<sub>3</sub>, Na<sub>2</sub>SO<sub>4</sub>, water glass and etc.) on the shrinkage is also related with the alkali concentration [34]. Moreover, Lahalle et al. [29] and Ye et al. [13] also investigated the effect of curing temperature on the shrinkage. A high curing temperature is beneficial to reduce the shrinkage, but could sharply decrease the setting time which brings another challenge in site construction.

Considering the difficulties in controlling the shrinkage of AAS, researchers start to seek for additives to mitigate the shrinkage in order to promote the application of alkali-activated slag, such as reactive MgO, gypsum, shrinkage reducing agent (SRA), etc. Yuan et al. [35] tried to add the anhydrite and quick lime as the expanding source into AAS. Via exploring the mitigating shrinkage mechanism, it was found that the alkali-activated slag with 8% expand additive could decrease the drying shrinkage from  $4.5 \times 10^{-4}$  to  $1.0 \times 10^{-4}$ . Blending the AAS with gypsum could effectively compensate the drying shrinkage due to the formation of ettringite and portlandite in the reaction products [2,36,37]. The role of gypsum also could be also attributed to reduce the weight loss while the content is below 5%. In addition, other studies [38–41] explored the use of SRA to modify AAS. These materials belong to high-molecular polymers having no impact on the mineralogical compositions of hardened pastes. Adding the SRA into cement-based materials could significantly reduce the early shrinkage. Jia et al. [42] evaluated the effect of various expansion agents (calcium sulpho-aluminate type and CaO type) on drying shrinkage. It was found that the formation of hydration products (Aft and CH) could reduce the drying shrinkage. Other studies [37,43,44] also found that the compensation effect on shrinkage was carried out due to the formation of Aft and AFm.

From the above review, the available researchers mainly focus on the effect of additive and the factors considered involve alkali content, modulus of alkali solution, gypsum, SRA, expansion agent, and etc. However, the effects of those strategies on the drying shrinkage of AAS are highly scattered in different studies, and it is difficult to make a reasonable comparison. Furthermore, the price of SRA additives is relatively high and its use will limit the application of alkali-activated slag. The combination of alkali solution and additives on shrinkage of alkali-activated slag are not systematically explored. This is also the original intention for designing this work. Hence, the effects of cement, alkali solution (alkali content and modulus of sodium silicates solution) and gypsum on the compressive strength, weight loss and drying shrinkage for alkali-activated slag cement were investigated in this study. The partial factor of combined activation on compressive strength and drying shrinkage with increasing the curing time also systematically evaluated. In the meantime, we also could use the results for regression analysis of partial factors to predict the shrinkage of alkali-activated slag mortar at different curing periods.

## 2. Materials and methods

### 2.1. Raw materials

The slag is the same materials used in [2] with specific surface area of 5000 cm<sup>2</sup>/g and density of 2920 kg/m<sup>3</sup>. Swedish Bascement (CEM II/A-V 52.5 N) was provided by Cementa. The properties of cement were shown in Table 1. Table 2 exhibits the chemical compositions of cement and slag by X-ray fluorescence (XRF) analysis. The mineralogical phases of cement and slag, which were determined via XRD analysis, the results are shown in Fig. 1. It is obvious from Fig. 1 that the main mineralogical phase of slag is amorphous. Meanwhile, the main crystalline phases of cement include C3S and C2S. Gypsum (CaSO<sub>4</sub>·2 H<sub>2</sub>O) was purchased from Fisher Scientific. The alkali solution was prepared by the sodium silicate solution with the moduli of 3.35 (provided by Sibelco Nordic), sodium hydroxide (NaOH, analytical grade with a purity ≥ 98.5%, Fisher Scientific, Sweden) and water. Choosing the natural sand with a size range of 0–4 mm as fine aggregates.

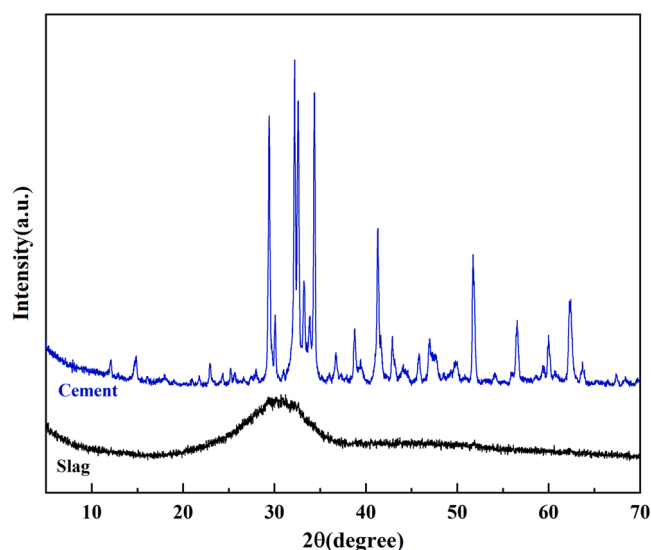
**Table 1**  
The basic properties of Bascement provided by manufacturer.

| Property                             | Bascement |
|--------------------------------------|-----------|
| Clinker content (%)                  | 80–94     |
| Fly ash content (%)                  | 6–20      |
| Compact density (kg/m <sup>3</sup> ) | 3000      |
| Bulk density (kg/m <sup>3</sup> )    | 1250      |
| Blaine fineness (m <sup>2</sup> /kg) | 450       |
| Alkali, Na <sub>2</sub> O (%)        | 1.1       |
| Gypsum (%)                           | 3.7       |
| Chloride, Cl <sup>-</sup> (%)        | 0.08      |
| Initial setting time (min)           | 150       |

**Table 2**

Chemical compositions of the cement and slag (wt%).

| Material | Oxide compositions |                  |                                |                 |                                |                  |      |                   |        |
|----------|--------------------|------------------|--------------------------------|-----------------|--------------------------------|------------------|------|-------------------|--------|
|          | CaO                | SiO <sub>2</sub> | Fe <sub>2</sub> O <sub>3</sub> | SO <sub>3</sub> | Al <sub>2</sub> O <sub>3</sub> | K <sub>2</sub> O | MgO  | Na <sub>2</sub> O | Others |
| Cement   | 64.50              | 22.50            | 4.00                           | 2.60            | 3.10                           | 0.58             | 1.30 | 0.12              | 1.30   |
| Slag     | 39.11              | 36.63            | 0.49                           | 0.27            | 13.56                          | 0.57             | 8.52 | 0.42              | 0.43   |

**Fig. 1.** Phase compositions of cement and slag.

## 2.2. Mixture design

**Table 3** lists the constitutions all prepared sample in this work. For all the mixtures, the fixed parameter of alkali-activated slag cement was the water to binder (w/b) ratio and sand to binder ratio, which are 0.5 and 3, respectively. The effect of alkali content (Na<sub>2</sub>O in mass % of binder), the molar ratio of water glass (Mr) or in other words the added silica content (SiO<sub>2</sub> in mass % of binder), and gypsum content (CaSO<sub>4</sub>·2 H<sub>2</sub>O in mass % of slag) on compressive strength, weight loss and drying shrinkage were explored. It is worth to notice that alkali and silica content were expressed by the ratio of the binder, while the gypsum content were given by the ratio of slag. The water glass, as the main activator, was involved in the hydration process and contributed to both the sodium and silica content. Moreover, the binder system includes the cement and the slag, as well as the gypsum. The total gypsum content includes the extra gypsum and gypsum content in cement, as shown in **Table 3**.

The proportion parameters were categorized into three groups: i) the slag to cement mass ratio (s/c) was chosen to be 100/0, 80/20 and 0/100 as reference. Although the main investigated s/c ratio was 80/20, there was a special testing group in which the s/c ratios

**Table 3**

The mixtures compositions of prepared AAS mortars.

| Sample ID        | Binder  |           | Alkali solution   |         | Gypsum, % | Sand/binder | w/b | Total Gypsum content, % |
|------------------|---------|-----------|-------------------|---------|-----------|-------------|-----|-------------------------|
|                  | Slag, % | Cement, % | Alkali content, % | Modulus |           |             |     |                         |
| Mr0C100N0G0      | 0       | 100       | 0                 | 0       | 0         | 3:1         | 0.5 | 3.70                    |
| Mr1.2C0N5G5      | 100     | 0         | 5                 | 1.2     | 5         | 3:1         | 0.5 | 5.00                    |
| Mr1.2C6N5G5      | 94      | 6         | 5                 | 1.2     | 5         | 3:1         | 0.5 | 5.22                    |
| Mr1.2C11N5G5     | 89      | 11        | 5                 | 1.2     | 5         | 3:1         | 0.5 | 5.50                    |
| Mr1.2C20N5G5     | 80      | 20        | 5                 | 1.2     | 5         | 3:1         | 0.5 | 5.74                    |
| Mr1.2C20N5G1.4   | 80      | 20        | 5                 | 1.2     | 1.4       | 3:1         | 0.5 | 2.14                    |
| Mr1.2C20N5G2.5   | 80      | 20        | 5                 | 1.2     | 2.5       | 3:1         | 0.5 | 3.24                    |
| Mr1.2C20N2.4G0   | 80      | 20        | 2.4               | 1.2     | 0         | 3:1         | 0.5 | 0.74                    |
| Mr1.2C20N2.4G2.5 | 80      | 20        | 2.4               | 1.2     | 2.5       | 3:1         | 0.5 | 3.24                    |
| Mr1.2C20N3G2.5   | 80      | 20        | 3                 | 1.2     | 2.5       | 3:1         | 0.5 | 3.24                    |
| Mr1.2C20N5G2.5   | 80      | 20        | 5                 | 1.2     | 2.5       | 3:1         | 0.5 | 3.24                    |
| Mr1.5C20N5G2.5   | 80      | 20        | 5                 | 1.5     | 2.5       | 3:1         | 0.5 | 3.24                    |
| Mr1.7C20N5G5     | 80      | 20        | 5                 | 1.7     | 5         | 3:1         | 0.5 | 3.24                    |

were 94/6 and 89/11. ii) the gypsum content (G) was defined as 0%, 1.4%, 2.5% and 5.0% of the slag content. iii) the added alkali content (N) was in the range of 2.4–5% and the binder usage is fixed, moduli of alkali solution, gypsum, sand/binder and w/b. Water glass with different molar ratios (Mr) was added to the mixture to adjust the material properties. For example, sample Mr1.2C20N5G5 means that the mixture contains a s/c ratio of 80/20 with 5% (in mass of slag content) of gypsum content and 5% (in mass of binder) of added Na<sub>2</sub>O content (N), 6% (in mass of binder) of added SiO<sub>2</sub> content (S) as the molar ratio (Mr) of water glass is 1.2. According to the results of previous researches, higher alkali content and modulus of sodium silicate solution would sharply increase the compressive strength of alkali-activated slag mortars, however, increasing the content of gypsum presents an opposite trend. Hence, this study explores the partial factors of combined activation (gypsum content, SiO<sub>2</sub> and Na<sub>2</sub>O) on strength development and drying shrinkage of alkali-activated slag mortar.

### 2.3. Specimen preparations

The water glass with a specified molar ratio were prepared prior to the preparation of the mortars to allow the water glass to reach thermal equilibrium. The role of NaOH solution was used to adjust the molar ratio of alkali solution to a certain value. The mixing and curing procedures for alkali activated slag cement were as follows:

- (I) The dry cementitious powders (slag, cement and gypsum) were blended in a mortar mixer for 1 minute. Then the alkali solution was added to the dry mixture and slowly blended for 30 s, and the sand was filled during the next 30 s;
- (II) The similar procedure as described in EN 196–1 was employed, that is, blending the paste at the high rate for 30 s, resting for 90 s and followed by one-minute blending at the high rate;
- (III) After the mixing, the mixture was casted into the mold with a dimension of 40 × 40 × 160 mm<sup>3</sup> and covered by a layer of plastic foil to prevent water evaporation during the first day of hydration. For each mixture, more than 12 specimens were casted in order to obtain an average value for both strength and drying properties;
- (IV) The specimens were taken out of the molds after 24 h in the mold and thereafter cured in water for the specific ages before testing.

### 2.4. Test methods

The mechanical and shrinkage tests were performed to exam the effect of different mixture proportions. According to EN 196–1, the compressive strength was measured at the age of 7, 28, 90 and 365 days. The drying shrinkage was measured repeatedly at certain time intervals during two years according to the standard ASTM C 596. The weight loss of specimens during the drying shrinkage process were tested by electronic balance at different curing time.

### 2.5. Methodology for partial factor of combined activation

The key object of this study is to identify the effects of different chemical compositions (silica and alkali content) on the strength and shrinkage developments. Therefore, the slag content (or s/c ratio), the silica content (S), the sodium content (N) and the gypsum content (G) were investigated.

The dissolving process of silica existed in slag is very slow. It is well known that adding additional silica is an effective solution to improve the early strength. In the meantime, the additional silica also increases the dry shrinkage of the concrete, which induced cracks and damaged the structure. Gypsum can be added into alkali-activated slag to form Na<sub>2</sub>SO<sub>4</sub>•10 H<sub>2</sub>O among hydration to reduce the dry shrinkage, as shown in Eq. (1).



Both qualitative and quantitative analysis on the effect of mixture parameters on properties of AAS mortars were conducted in this work. The qualitative analysis was based on comparative study, where only one variable was investigated, and other parameters were kept constant. The quantitative analysis was carried out to evaluate the contribution of each mixture parameter, by means of regression analysis. According to the fundamentals of cement chemistry, each additional component contributes to the performance development differently. In order to evaluate the contribution of different components to the strength development, a concept of "partial factor" of equivalent activation was adopted here. This concept is similar with the partial factor when the water to binder (w/b) ratio is calculated. Therefore, using the concept of partial factor of equivalent activation ( $\gamma$ ), a combined activation (CA) can be calculated and used for proportion design.

The principle is to consider the partial factor of added alkali as 1. For other added components, the partial factors were decided based on empirical experience and experimental data. The partial factor indicates how much an additional component contributes to a certain material property which can also be used as a design tool to tailor the concrete properties. The combined activation (CA) can be expressed as:

$$\text{CA} = \gamma_a \times N + \gamma_s \times S + \gamma_g \times G \quad (2)$$

where  $\gamma_a$  is the partial factor of added alkali which equals 1;  $\gamma_s$  and  $\gamma_g$  stand for the partial factors of added silica and gypsum which were decided by experimental data;  $N$  for the content of added alkali (Na<sub>2</sub>O) in mass of binder;  $S$  for the content of added silica (SiO<sub>2</sub>) in

mass of binder;  $G$  for the content of added gypsum ( $\text{CaSO}_4 \cdot 2\text{H}_2\text{O}$ ) in mass of slag.

### 3. Results and discussion

#### 3.1. Compressive strength of alkali-activated slag mortar

##### 3.1.1. Effect of cement content

Fig. 2 presents the compressive strength evolution of Portland cement mortar (Mr0C100N0G0) and alkali-activated slag mortar added with various cement content in water curing. Furthermore, specimen Mr0C100N0G0 was used as blank to compare the effect of cement on alkali-activated slag mortars. The compressive strength of all specimens gradually increases with extending the curing period. Compared to the alkali-activated slag, the compressive strength of Mr0C100N0G0 is higher at the same curing age. For instance, the compressive strength of specimen Mr0C100N0G0 at 7 days is 40.48 MPa, while that of Mr1.2C0N5G5, Mr1.2C6N5G5, Mr1.2C11N5G5 and Mr1.2C20N5G5 exhibits a decrease of 27.1%, 7.1%, 9.2% and 22.6%, respectively. It is apparent that the compressive strength of alkali-activated slag mortar with the same alkali and silica content is firstly increased and then decreased with the increase of cement content from 0 to 20 wt%, and reaches the maximum value when the addition of cement is 11 wt%. Furthermore, the increasing rate of compressive strength is higher in the first 90 days, and then becomes gentle. The alkali provided by the cement could effectively promote the secondary hydration of slag. In the early stage, the alkali-activated slag possesses lower strength than ordinary Portland cement pastes. The reason is that the role of slag with lower reactivity mainly is to fill the voids and compact the matrix during the early hydration process. The slag can be activated by alkali solution and  $\text{Ca}(\text{OH})_2$  at late age [11,45]. In the meantime, the secondary hydration of slag will improve the formation of C-S(A)-H gel with a low Ca/Si ratio, and also contribute to the development of compressive strength and the volume stability [46].

##### 3.1.2. Effect of gypsum content

Fig. 3 shows the effect of gypsum content on compressive strength evolution of alkali-activated slag mortar. The compressive strength development of all specimens firstly increases and then decreases with the increased gypsum content from 0 to 5 wt%, and reaches the maximum value while the addition of gypsum content is 1.4 wt%. Compared to the specimen Mr0C100N0G0, the largest compressive strength value of 74.1 MPa is achieved after 365 days curing. When the gypsum content was 1.4 wt%, compressive strength of alkali-activated slag mortar after 365 days curing would increase a little and increase from 71.07 MPa to 74.08 MPa. However, the compressive strength of mortars decreased by 14.2% and 24.0% respectively while the gypsum contents were 2.5 wt% and 5 wt%. Similar results were also obtained in the previous studies, that is, adding a small amount of gypsum into the alkali-activated materials could slight increase the compressive strength [2,36,47,48]. The reason is that the gypsum could provide extra  $\text{Ca}^{2+}$ , which could react with silicate and aluminosilicate group to form C-S-H and strengthen the compressive strength. The geopolymerization process of alkali-activated slag will be obstructed when the gypsum addition is higher than 1.4 wt%, which also drastically decreases the strength.

##### 3.1.3. Effect of alkali content

The compressive strengths of alkali-activated slag mortar with various alkali contents at 7, 28, 90 and 365 days are given in Fig. 4. The results show that the alkali content plays a crucial role in determining the development of compressive strength for alkali-activated slag. In the meantime, using higher alkali content is beneficial to the development of compressive strength, which is in agreement with

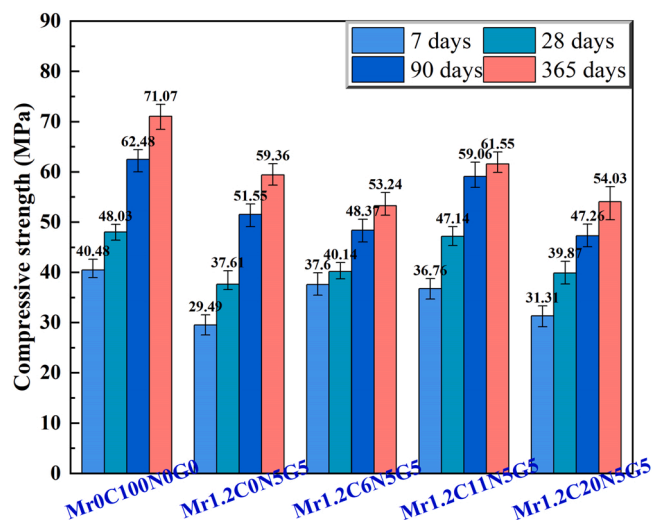


Fig. 2. Effect of cement content on compressive strength.

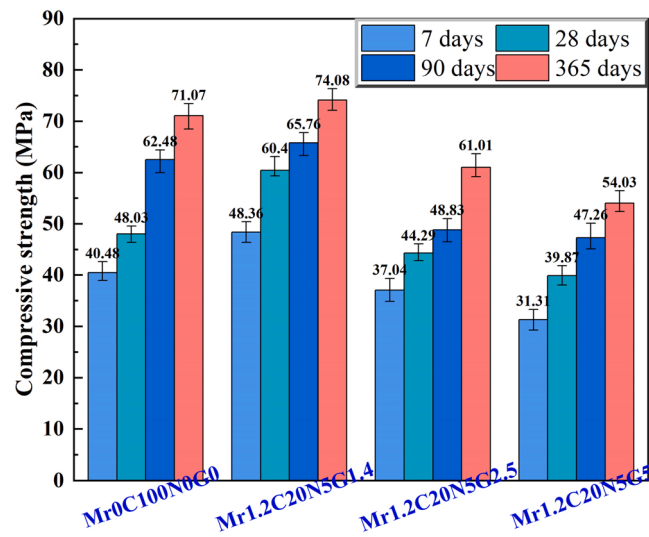


Fig. 3. Effect of gypsum content on compressive strength.

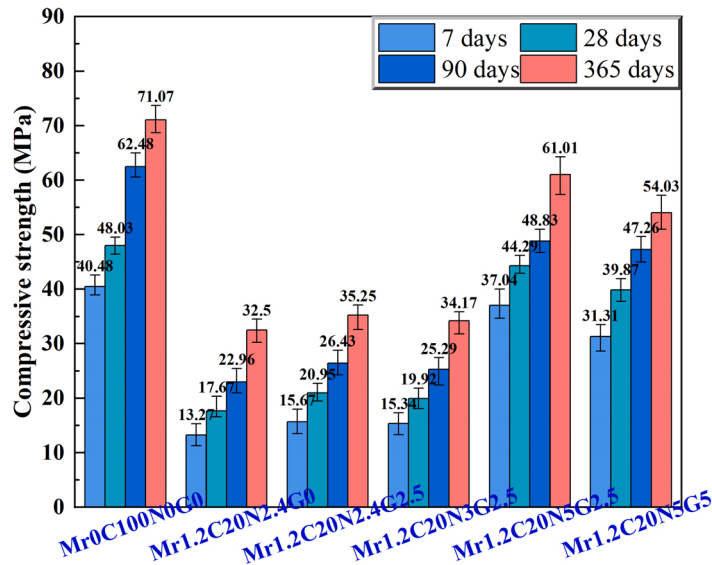


Fig. 4. Effect of alkali content on compressive strength.

the observations from the previous studies [31,49–51]. It is noted that although increasing the alkali content could increase the compressive strength of all alkali-activated slag mortars, which is still lower than that of Mr0C100N0G0 due to the lower reactivity of slag. Furthermore, Mr1.2C20N2.4G0 and Mr1.2C20N2.4G2.5, adding a small amount of gypsum could slightly increase the strength of alkali-activated slag mortar. Keeping the gypsum content at 2.5 wt%, the compressive strength only has a little change as the alkali content increases from 2.4 to 3 wt% during the whole curing period. However, specimen with a higher strength can be realized with increasing continuously the alkali content from 3 to 5 wt%. Especially after 365 days of curing, there is a sharp increase in the compressive strength for alkali-activated slag mortar, which increases from 34.2 to 61.0 MPa.

#### 3.1.4. Effect of modulus of sodium silicate solution

By correlating the modulus of sodium silicate solution with the measured compressive strengths of alkali-activated slag mortar as shown in Fig. 5, it can be found that the compressive strength of alkali-activated slag mortar prepared with various moduli of sodium silicate solution shows an increase trend within a certain curing period. The reason is that increasing the silica content in alkali solution would decrease the Ca/Si ratio of C-S(A)-H. At the same time, this will decrease the molar volume of the C-S(A)-H and increase the surface areas of C-S(A)-H, which could be one of the reasons explain the improved compressive strength [49,52]. It is obvious that increasing the modulus of sodium silicate solution from 1.2 to 1.5 is in favor of the development of compressive strength during the



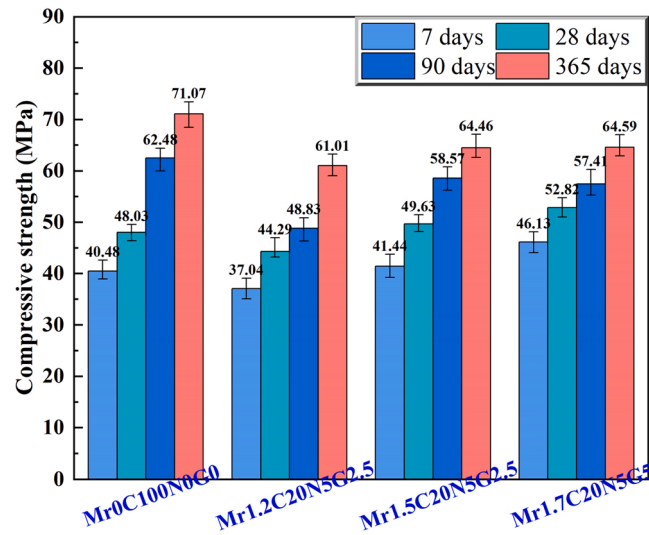


Fig. 5. Effect of moduli of sodium silicate solution on compressive strength.

whole curing period. Increasing the modulus of sodium silicate solution from 1.5 to 1.7 furtherly enhances the 7 and 28 days compressive strength even though the gypsum content was increased from 2.5 to 5 wt%. Furthermore, it is easily found that increasing modulus of sodium silicate solution only has little influence on the strength after 365 days. Compared to the strength of Mr1.2C20N2.4G5 (Fig. 4), alkali-activated slag mortar with gypsum content of 5 wt%, the strength increases with the modulus of sodium silicate solution, particularly for the modulus of sodium silicate solution from 1.2 to 1.7. The increasing trend of compressive strength for alkali-activated slag mortar with the alkali modulus from 1.2 to 1.7 gradually decreases with the extension of the curing period from 7 to 365 days, which are 47.4%, 32.5%, 21.5% and 19.5%, respectively.

### 3.2. Drying shrinkage of alkali-activated slag mortar

#### 3.2.1. Effect of cement content

Drying shrinkage of alkali-activated slag cement with various cement contents is shown in Fig. 6. It can be clearly seen from Fig. 6 that drying shrinkage of alkali-activated slag mortar ranges from  $30 \times 10^{-4}$  to  $45 \times 10^{-4}$  after 778 days, which are higher than that of cement mortar Mr0C100N0G0 ( $10.4 \times 10^{-4}$ ). Most of shrinkage of alkali-activated slag mortar occurred within the early age, especially for the specimen Mr1.2C0N5G5. The results show that the drying shrinkage of alkali-activated slag mortar increases by 3–5 times larger as much as that of Mr0C100N0G0, which gradually decreases with the addition of cement from 0 to 20 wt%. The reason is that the majority pores in the sample are in the micro size in compared with that of Mr0C100N0G0 [53]. This is well agreed with the

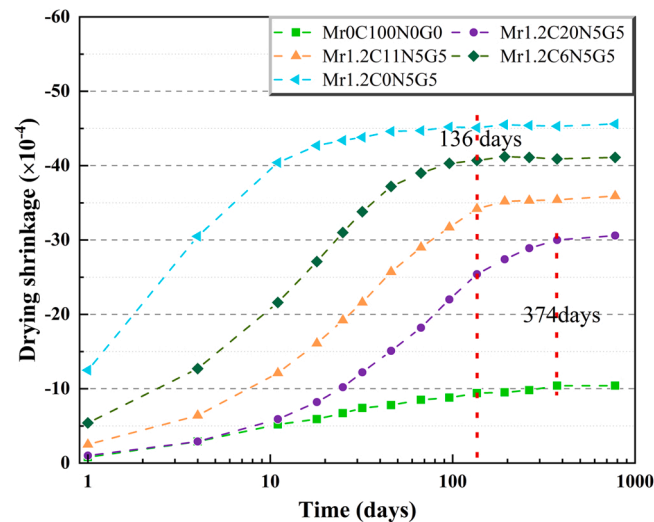


Fig. 6. Effect of cement content on drying shrinkage.



previous studies [49,51,54]. Furthermore, the pore size distributions and hydration products between Portland cement and alkali-activated slag are also different [24,28,55]. Drying shrinkage of specimen Mr1.2C0N5G5 reaches a plateau after 14 days, and the time for reaching a stable value is delayed with increasing the cement content, which is consistent with the results reported by Liu et al. [2]. While the addition of cement is below 20 wt%, the total drying shrinkage reaches a stable state after 136 days. The stable state of specimens Mr0C100N0G0 and Mr1.2C20N5G5 will be prolonged to 374 days although the total drying shrinkage is lower than the other specimens.

### 3.2.2. Effect of gypsum content

Previous studies found that the total gypsum content within concrete should be limited in approximately 5 wt% due to the fact that the concrete with higher sulphate dosage will easily show a volume expansion and crack [37]. Fig. 7 presents the effect of gypsum content on drying shrinkage for alkali-activated slag mortar. Therefore, the gypsum content was chosen from 0 to 5 wt% for avoiding the volume expansion and cracks in this work.

The drying shrinkage of alkali-activated slag mortar demonstrates the same trend although the addition of gypsum content ranging from 1.4 to 5 wt%. Furthermore, the total drying shrinkage gradually decreases as the increasing of the gypsum content. For instance, the drying shrinkage of specimens after 778 days with the increasing of gypsum content from 2.4 to 5 wt% are  $33.5 \times 10^{-4}$ ,  $32.3 \times 10^{-4}$  and  $30.6 \times 10^{-4}$ , respectively. Several factors can be considered for this phenomenon: (1) gypsum with the expansion potential is effective in compensating the drying shrinkage [44,56]; (2) the gypsum could reacts with alkali and  $Al_2O_3$  from slag to form portlandite and ettringite to compensate the drying shrinkage, which is in agreement with other works [43,57].

### 3.2.3. Effect of alkali content

The drying shrinkage of alkali-activated slag mortar with various alkali contents are given in Fig. 8. As shown in Fig. 8, the total drying shrinkage of Mr0C100N0G0, Mr1.2C20N2.4G0, Mr1.2C20N2.4G2.5 and Mr1.2C20N3G2.5 remains approximately at the same level before 67 days. The drying shrinkage of specimens Mr1.2C20N2.4G0 and Mr1.2C20N2.4G2.5 with the same alkali content, cement content and modulus of sodium silicate solution show only a little change with increasing the gypsum content from 0 to 2.5 wt%. Furthermore, it is obvious that the alkali content increased from 2.4 to 3.0 wt% has no significant influence on the shrinkage. The drying shrinkage increases sharply from  $19.2 \times 10^{-4}$  to  $32.3 \times 10^{-4}$  with an increase of alkali content from 3 and 5 wt% although the gypsum content of 2.5 wt% was added into the matrix [58]. Increasing the addition of gypsum from 2.5 to 5 wt% could not compensate the total drying shrinkage of specimens Mr1.2C20N5G2.5 and Mr1.2C20N5G5 with the alkali content of 5 wt%. In this case, adding the gypsum into alkali-activated slag has an obvious impact on the drying shrinkage while the matrix possesses the similar alkali content. The reason is that using a higher alkali content leads to an increased slag particle reaction degree, which could increase the surface tension of pore solution and decrease the humidity of specimens. These factors combined could increase the capillary stress.

### 3.2.4. Effect of modulus of sodium silicate solution

Fig. 9 shows the effect of modulus of sodium silicate solution on drying shrinkage of alkali-activated slag mortar. Compared with the results of specimen Mr0C100N0G0, the total drying shrinkage of alkali-activated slag mortar (Mr1.2C20N5G2.5 and Mr1.5C20N5G2.5) is higher with the increased modulus of sodium silicate solution from 0 to 1.5. Furthermore, the shrinkage only changes a little with the modulus of sodium silicate solution increased from 1.2 to 1.5 under the same alkali content of 5%. Previous studies [28,59,60] pointed out that the modulus of sodium silicate solution had negative impact on the drying shrinkage, which could provide large amount of silicate ions for the geopolymerization of C-S-H gels with lower C/S ratio. The low C/S ratio of C-S-H could

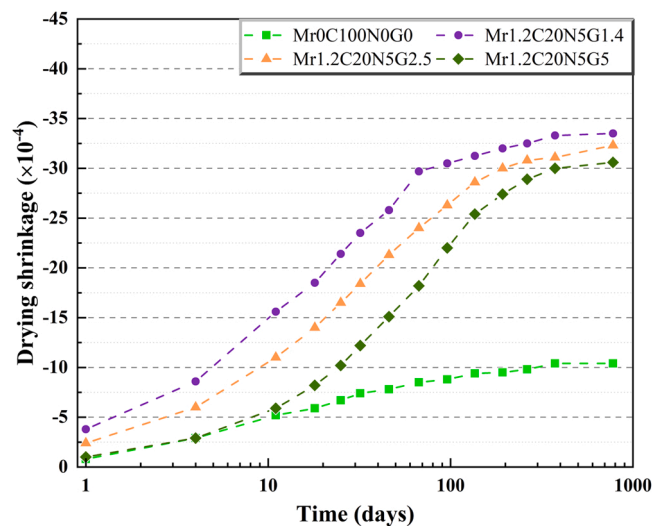


Fig. 7. Effect of gypsum content on drying shrinkage.

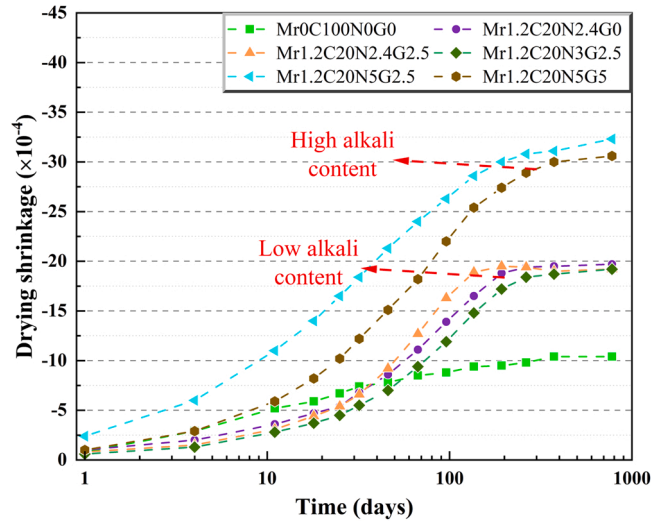


Fig. 8. Effect of alkali content on drying shrinkage.

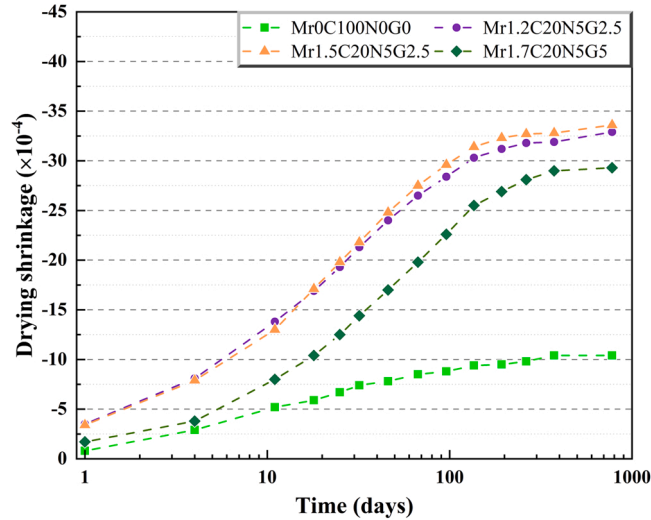


Fig. 9. Effect of moduli of sodium silicate solution on drying shrinkage.

increase shrinkage in a dry environment. The total drying shrinkage of Mr1.2C20N5G2.5 and Mr1.7C20N5G5 after drying for 778 days are  $32.9 \times 10^{-4}$  and  $29.3 \times 10^{-4}$ , respectively. By comparing the results of drying shrinkage for Mr1.2C20N5G2.5 and Mr1.7C20N5G5, it was found that increasing the gypsum content from 2.5 to 5 wt% could compensate the shrinkage although the modulus of sodium silicate solution has increased from 1.2 to 1.7.

### 3.3. Weight loss of alkali-activated slag cement

#### 3.3.1. Effect of cement content

The effect of cement content on weight loss for alkali-activated slag mortar is shown in Fig. 10. The weight loss can be an important factor to evaluate the drying shrinkage, which also is related to the change in humidity above the curved meniscus surface of the capillary water in the pores and partially adsorbed water in the surfaces of hydration products [27]. It is clear that the weight loss of specimens gradually increase with increasing the cement content from 0 to 20 wt%. Furthermore, the total weight loss of all alkali-activated slag mortar is higher than the OPC mortar after 778 days. The total weight losses of specimens are 4.17%, 4.34%, 4.71% and 4.74%, respectively with increase of the cement content from 0 to 20 wt%, while the value of OPC mortar is 3.64%. However, the weight loss of Mr1.2C0N5G5 and Mr1.2C6N5G5 is smaller than that of OPC mortar before 67 days, then became a slow increasing rate with curing.

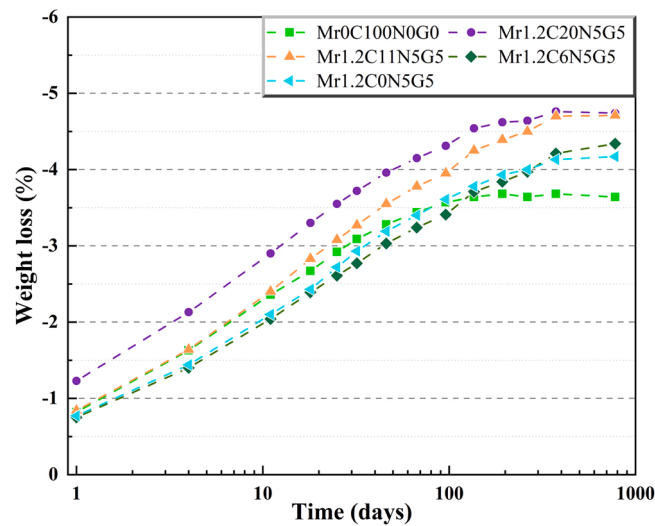


Fig. 10. Effect of cement content on weight loss.

### 3.3.2. Effect of gypsum content

Fig. 11 presents the results showing the effect of gypsum content on weight loss. It can be seen that the weight losses of alkali-activated slag mortar firstly decrease and then increase with the increased gypsum content from 1.4 to 5 wt%. In the meantime, the weight losses of specimens Mr1.2C20N5G1.4 and Mr1.2C20N5G2.5 are lower than that of OPC mortar when the gypsum content is below 2.5 wt%. This is opposite to the results of drying shrinkage. The reason is that a certain quantity of ettringite with porous structure is able to store more amount of water which could reduce the evaporation under a drying environment. When the amount of ettringite exceeds a critical level, it will increase the evaporation resulting in a higher water loss. This observation is in agreement with the findings reported by the previous researches [2,33,61]. The weight loss of alkali-activated specimens will increase when the addition of gypsum is over 2.5 wt%.

### 3.3.3. Effect of alkali content on weight loss

Fig. 12 presents the effect of alkali content on weight loss for alkali-activated slag mortar. The total weight losses of alkali-activated slag mortar are higher than that of OPC mortar except for the specimen Mr1.2C20N5G2.5. Increasing the alkali content from 2.4 to 5 wt% has a significantly influence on the weight loss while the addition of gypsum content is 2.5 wt%. The main reason is that increasing the alkali content significantly increased the hydration degree of slag, leading to a higher strength, as shown in Fig. 3. It is well known that an increased degree of hydration implies a decreased free water in the mortar [49]. While the alkali content is at 5 wt%, increasing the gypsum content from 2.5 to 5.0 wt% will increase the weight loss from 3.10% to 4.17%. Increasing the gypsum content from 0 to 2.5 wt% only has a little influence on the weight loss of the specimen with lower alkali content of 2.4 wt%.

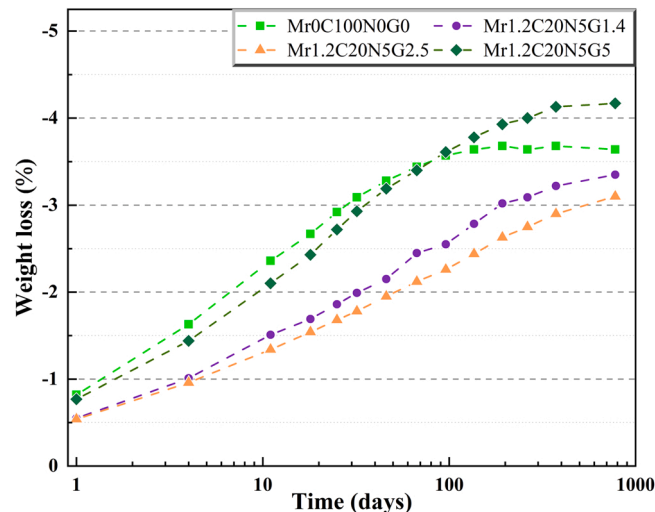


Fig. 11. Effect of gypsum content on weight loss.

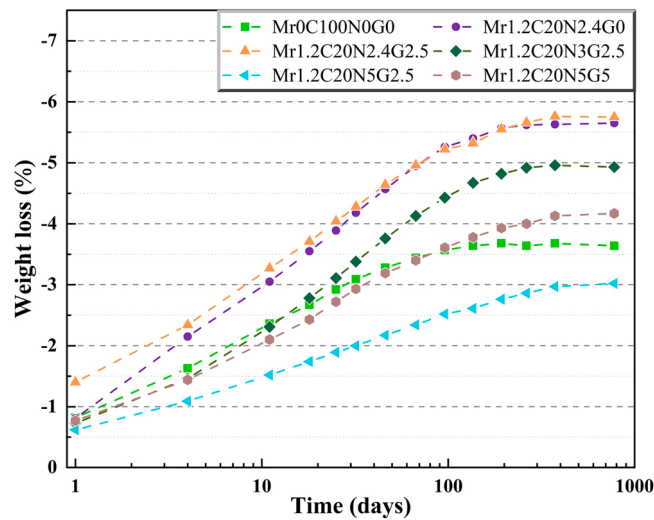


Fig. 12. Effect of alkali content on weight loss.

### 3.3.4. Effect of modulus of sodium silicate solution

The effect of modulus of sodium silicate solution on weight loss for alkali-activated slag mortar is shown in Fig. 13. It can be found that the weight losses of specimens gradually decreased from 4.17% to 3.8% with increasing the modulus of sodium silicate solution from 1.2 to 1.5 while the addition of gypsum content is 2.5 wt%. Compared with the results of drying shrinkage and weight loss, it can be found that the weight loss is positively proportional to the drying shrinkage (Figs. 5 and 9). For Mr1.2C20N5G5 (Fig. 12) and Mr1.7C20N5G5 their weight losses only vary a little when increasing the modulus of sodium silicate solution from 1.2 to 1.7 while the addition of gypsum content is at 5 wt%.

## 3.4. Partial factor analysis

### 3.4.1. Partial factors of combined activation on strength development

The objective of increasing the additional alkali content is in favor of activating the slag hydration degree, and also beneficial for dissolving solid silica into ions. In other words, the dissolution process of silica gradually increases with the increase of alkali concentration. However, higher alkali content will hinder the dissolution of calcium ions which is detrimental for the formation of C-S-H gel, and eventually impact the development of strength. Therefore, the alkali content needs to be controlled within a reasonable range. According to our previous testing, if the added alkali content reached 8%, the setting time sharply decreases to about few minutes. Too short setting time makes it very difficult even impossible in site construction. Hence, in this study, the added alkali content was chosen between 2.4% and 6%, to ensure an efficient activation and enough setting time.

According to regression analysis of compressive strength at 28 days, the partial factors  $\gamma_s$  and  $\gamma_g$  were determined as 0.3 and  $-0.3$ , respectively. The physical meanings are that increasing the content of silica has positive effect on strength, while gypsum content has negative effect. Therefore, the compressive strength ( $f_c$ ) can be predicted with known mixture proportions using:

$$f_c = a \times CA + b \quad (4)$$

where CA is the combined activation factor that can be calculated by Eq. 2, a and b are regression constants.

Fig. 14 illustrates the regression results of alkali-activated slag mortar at 28 days, 90 days and 365 days with  $\gamma_s$  and  $\gamma_g$  as 0.3 and  $-0.3$ , respectively. From Fig. 14, it is obvious that the relationships between compressive strength and combined activation show a well linear trend. Furthermore, the regression analysis achieves good correlation with the test data, where the  $R^2$  was 0.9848, 0.9749 and 0.9691 at 28, 90 and 365 days, respectively.

The regression constants of compressive strength ( $f_c$ ) in relation with the combined activation factor (CA) are listed in Table 4. Thus, the compressive strength at 28 days and 90 days can be estimated accordingly.

### 3.4.2. Partial factors of combined activation on shrinkage

Fig. 15 shows the regression analysis of partial factors on the effects for shrinkage development. Partial factor  $\gamma_a$  stands for the effect of alkali content on shrinkage,  $\gamma_s$  for the effect of silica content and  $\gamma_g$  for the effect of gypsum content. Different from those for strength development, the partial factors for shrinkage development are time-dependent. As shown in Fig. 15, all three partial factors varied very much in the first three months, after that they became stable. The physical meaning of the shrinkage partial factor is that positive values, such as for  $\gamma_g$ , have shrinkage reduction effect which is desirable in engineering design, while negative values, such as for  $\gamma_a$  and  $\gamma_s$ , indicate shrinkage enlargement which can cause problems such as cracking.

From the partial factor analysis, the conclusion could be obtained that gypsum can compensate the shrinkage caused by silica and

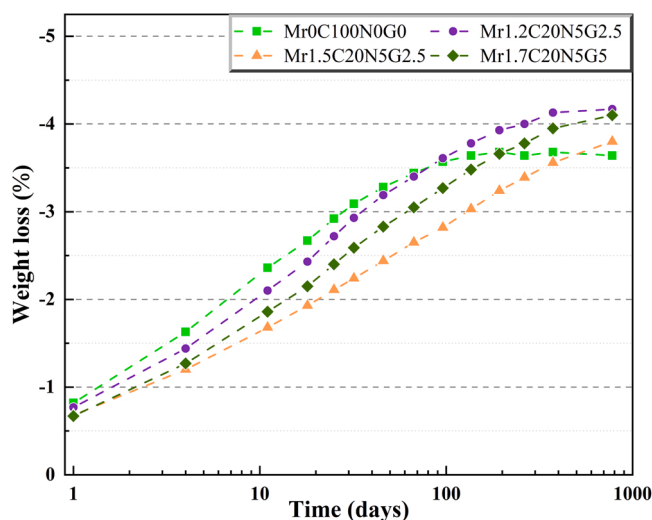


Fig. 13. Effect of moduli of sodium silicate solution on weight loss.

alkali content. However, the shrinkage reduction only happened in the early hydration stage, especially in the first 90 days. Furthermore, it showed that increasing the silica content would result in a larger shrinkage. Therefore, the content of silica should be limited during alkali activation, which in our study, we recommended the silica content ( $\text{SiO}_2$ ) should be around 5–6% in mass of the binder. It is noted that the silica content should be retrieved from the water glass content.

#### 4. Conclusions

Based on the results of compressive strength, drying shrinkage and weight loss for alkali-activated slag mortar determined by various cement contents, alkali contents, gypsum contents and modulus of alkali solution, we systematically deduced the partial factors for quantification of the effects on compressive strength and shrinkage development. This work lay a solid foundation for the green cementitious materials preparation, the factors analysis also contributes to the performance adjustment. The following conclusions can be drawn based on the test and analysis results:

- (1) Addition of cement in the alkali-activated slag has a positive impact on compressive strength, drying shrinkage and weight loss of alkali-activated slag mortar. Specimens with a higher cement content possess a higher strength, lower drying shrinkage and weight loss. Increasing the cement content from 0 to 20 wt%, the total drying shrinkage of specimens decreased from  $45 \times 10^{-4}$  to  $30 \times 10^{-4}$  after drying for 778 days. It should be kept in mind that addition of cement will increase the environmental impact.
- (2) Gypsum can effectively reduce the drying shrinkage especially at the early age up to three months. However, it has a negative impact on compressive strength of alkali-activated slag mortar.
- (3) Both alkali and silica positively contribute to compressive strength of alkali-activated slag mortar, but the contribution of silica is about 1/3 as much as alkali. However, both alkali and silica induce drying shrinkage, especially silica, which induces more than double as much as alkali. For the balance of compressive strength and drying shrinkage control, the alkali and silica content should be around 5–6% by mass of binder, implying a modulus of water glass about 1.
- (4) The contribution of various chemical components on drying shrinkage varies over time. The most significant positive effect of gypsum on shrinkage reduction occurred during the first 10–100 days of drying, in which alkali and silica have the largest shrinkage.

Compared to previous works, we also could study the comprehensive effects of expand agents, shrinkage reducing agents, supplementary cementing materials and raw materials composition for alkali activated slag on shrinkage in the future. Hence, avoiding the propagation of concrete structure.

#### CRedit authorship contribution statement

**Shunfeng Wang:** Investigation, Conceptualization, Writing – original draft, Data curation. **Kai Wu:** Visualization, Data curation. **Zhenghong Yang:** Investigation, Visualization, Data curation, Supervision. **Luping Tang:** Data curation, Supervision, Writing - review & editing.

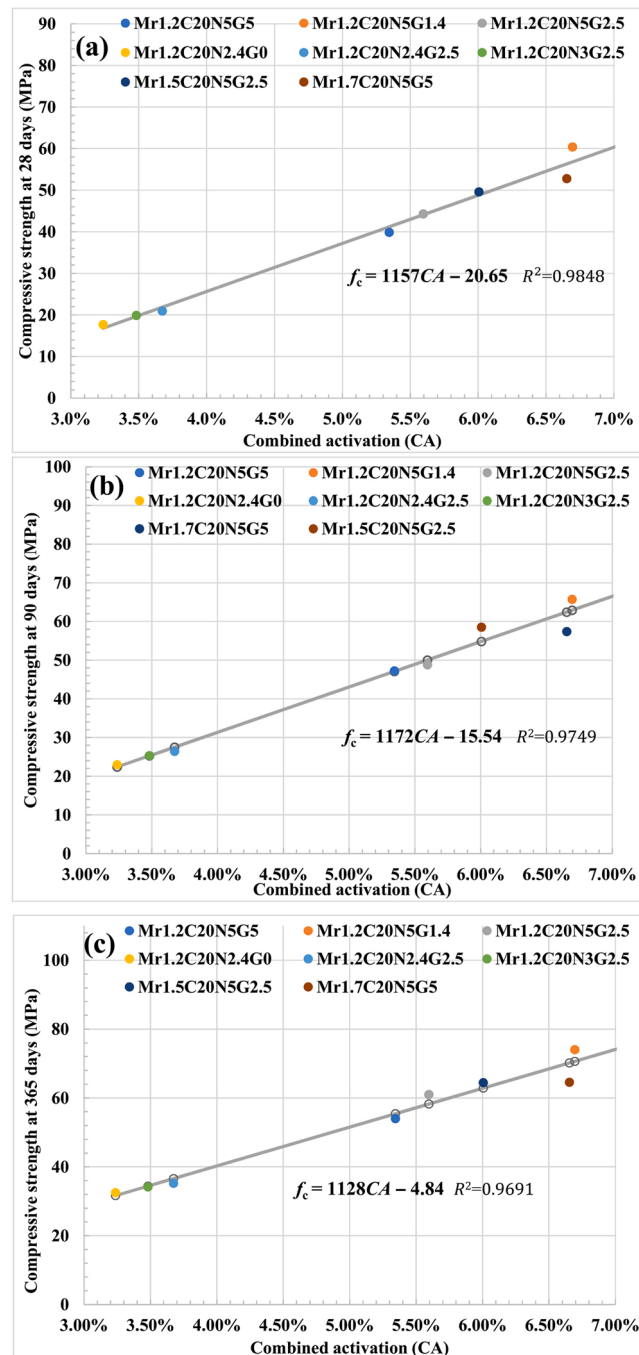


**Fig. 14.** Compressive strength in relation with the combined activation (CA) at (a) 28 days, (b) 90 days and (c) 365 days, with partial factors  $\gamma_s = 0.3$  and  $\gamma_g = -0.3$ .

**Table 4**

Regression analysis of compressive strength ( $f_c$ ) in relation with the combined activation (CA), with partial factors  $\gamma_s = 0.3$  and  $\gamma_g = -0.3$ . Noted that  $\gamma_a$  equals to 1.

|                          | Slope $a$ | Intercept $b$ | $R^2$  |
|--------------------------|-----------|---------------|--------|
| $f_{c,28 \text{ days}}$  | 1157      | -20.65        | 0.9848 |
| $f_{c,90 \text{ days}}$  | 1172      | -15.54        | 0.9749 |
| $f_{c,365 \text{ days}}$ | 1128      | -4.84         | 0.9691 |

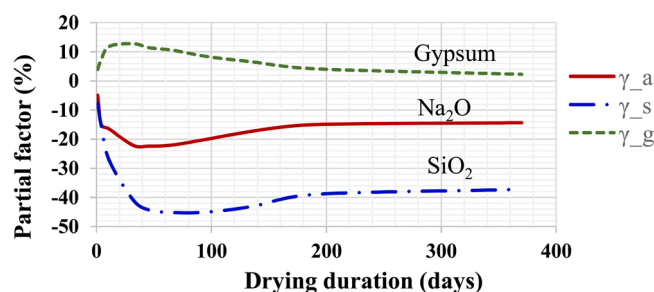


**Fig. 15.** Partial factors of shrinkage development. Partial factor  $\gamma_a$  stands for the effect of alkali content on shrinkage,  $\gamma_s$  for the effect of silica content and  $\gamma_g$  for the effect of gypsum content.

### Declaration of Competing Interest

The authors declare that they have no known competing financial interests or personal relationships that could have appeared to influence the work reported in this paper.

### Data Availability

No data was used for the research described in the article.

### Acknowledgments

The authors are grateful for the financial supports from Swedish VINNOVA (No. 2016-03367) and the China Scholarship Council (202106260096).

### References

- [1] M. Schneider, The cement industry on the way to a low-carbon future, *Cem. Concr. Res.* 124 (2019), 105792, <https://doi.org/10.1016/j.cemconres.2019.105792>.
- [2] J. Liu, L. Hu, L. Tang, E.Q. Zhang, J. Ren, Shrinkage behaviour, early hydration and hardened properties of sodium silicate activated slag incorporated with gypsum and cement, *Constr. Build. Mater.* 248 (2020), 118687, <https://doi.org/10.1016/j.conbuildmat.2020.118687>.
- [3] S. Zuo, Q. Yuan, T. Huang, K. Zhang, J. Shi, Y. Tan, Microstructural changes of young cement paste due to moisture transfer at low air pressures, *Cem. Concr. Res.* 164 (2023), 107061, <https://doi.org/10.1016/j.cemconres.2022.107061>.
- [4] K. Zhang, Q. Yuan, T. Huang, S. Zuo, H. Yao, Utilization of novel stranded steel fiber to enhance fiber–matrix interface of cementitious composites, *Constr. Build. Mater.* 369 (2023), 130525, <https://doi.org/10.1016/j.conbuildmat.2023.130525>.
- [5] Z. Wang, Y. Chen, L. Xu, Z. Zhu, Y. Zhou, F. Pan, K. Wu, Insight into the local C-S-H structure and its evolution mechanism controlled by curing regime and Ca/Si ratio, *Constr. Build. Mater.* 333 (2022), 127388, <https://doi.org/10.1016/j.conbuildmat.2022.127388>.
- [6] S. Wang, L. Yu, L. Huang, K. Wu, Z. Yang, Incorporating steel slag in the production of high heat resistant FA based geopolymer paste via pressure molding, *J. Clean. Prod.* 325 (2021), 129265, <https://doi.org/10.1016/j.jclepro.2021.129265>.
- [7] S.-D. Wang, X.-C. Pu, K.L. Scrivener, P.L. Pratt, Alkali-activated slag cement and concrete: a review of properties and problems, *Adv. Cem. Res.* 7 (1995) 93–102, <https://doi.org/10.1680/adcr.1995.7.27.93>.
- [8] S. Wang, L. Yu, F. Yang, W. Zhang, L. Xu, K. Wu, L. Tang, Z. Yang, Resourceful utilization of quarry tailings in the preparation of non-sintered high-strength lightweight aggregates, *Constr. Build. Mater.* 334 (2022), 127444, <https://doi.org/10.1016/j.conbuildmat.2022.127444>.
- [9] X. Zheng, H. Liu, S. You, S. Easa, K. Cheng, Z. Chen, T. Ji, Cracking resistance and sustainability assessment of alkali-activated slag concrete incorporating lightweight aggregate, *Cem. Concr. Compos.* 131 (2022), 104556, <https://doi.org/10.1016/j.cemconcomp.2022.104556>.
- [10] S. Narimani Zamanabadi, S.A. Zareei, P. Shoaee, F. Ameri, Ambient-cured alkali-activated slag paste incorporating micro-silica as repair material: Effects of alkali activator solution on physical and mechanical properties, *Constr. Build. Mater.* 229 (2019), 116911, <https://doi.org/10.1016/j.conbuildmat.2019.116911>.
- [11] G. Li, W. Wang, G. Zhang, Effects of slag on the degradation mechanism of ordinary Portland cement-calcium aluminate cement-gypsum ternary binder under the multiple erosive ions, *Constr. Build. Mater.* 324 (2022), 126661, <https://doi.org/10.1016/j.conbuildmat.2022.126661>.
- [12] J. Zhang, Y. Ma, J. Zheng, J. Hu, J. Fu, Z. Zhang, H. Wang, Chloride diffusion in alkali-activated fly ash/slag concretes: Role of slag content, water/binder ratio, alkali content and sand-aggregate ratio, *Constr. Build. Mater.* 261 (2020), 119940, <https://doi.org/10.1016/j.conbuildmat.2020.119940>.
- [13] H. Ye, A. Radlińska, Shrinkage mitigation strategies in alkali-activated slag, *Cem. Concr. Res.* 101 (2017) 131–143, <https://doi.org/10.1016/j.cemconres.2017.08.025>.
- [14] Y.X. Chen, G. Liu, K. Scholbach, H.J.H. Brouwers, Development of cement-free bio-based cold-bonded lightweight aggregates (BCBLWAs) using steel slag and miscanthus powder via CO<sub>2</sub> curing, *J. Clean. Prod.* 322 (2021), 129105, <https://doi.org/10.1016/j.jclepro.2021.129105>.
- [15] K. Tian, Y. Wang, S. Hong, J. Zhang, D. Hou, B. Dong, F. Xing, Alkali-activated artificial aggregates fabricated by red mud and fly ash: Performance and microstructure, *Constr. Build. Mater.* 281 (2021), 122552, <https://doi.org/10.1016/j.conbuildmat.2021.122552>.
- [16] S. Wang, L. Yu, L. Xu, K. Wu, Z. Yang, The failure mechanisms of precast geopolymer after water immersion, *Materials* 14 (2021) 5299, <https://doi.org/10.3390/ma14185299>.
- [17] S. Wang, X. Ma, L. He, Z. Zhang, L. Li, Y. Li, High strength inorganic-organic polymer composites (IOPC) manufactured by mold pressing of geopolymers, *Constr. Build. Mater.* 198 (2019) 501–511, <https://doi.org/10.1016/j.conbuildmat.2018.11.281>.
- [18] W. Chen, B. Li, J. Wang, N. Thom, Effects of alkali dosage and silicate modulus on autogenous shrinkage of alkali-activated slag cement paste, *Cem. Concr. Res.* 141 (2021), 106322, <https://doi.org/10.1016/j.cemconres.2020.106322>.
- [19] A.A. Abadel, H. Alghamdi, Effect of high volume tile ceramic wastes on resistance of geopolymer mortars to abrasion and freezing-thawing cycles: Experimental and deep learning modelling, *S0272884223000901*, *Ceram. Int.* (2023), <https://doi.org/10.1016/j.ceramint.2023.01.089>.



- [20] A. Mohsen, M. Kohail, A.A. Abadel, Y.R. Alharbi, M.L. Nehdi, M. Ramadan, Correlation between porous structure analysis, mechanical efficiency and gamma-ray attenuation power for hydrothermally treated slag-glass waste-based geopolymer, *Case Stud. Constr. Mater.* 17 (2022), e01505, <https://doi.org/10.1016/j.cscm.2022.e01505>.
- [21] P.S. Deb, P. Nath, P.K. Sarker, Drying shrinkage of slag blended fly ash geopolymer concrete cured at room temperature, *Procedia Eng.* 125 (2015) 594–600, <https://doi.org/10.1016/j.proeng.2015.11.066>.
- [22] G.F. Huseien, M.A. Asaad, A.A. Abadel, S.K. Ghoshal, H.K. Hamzah, O. Benjeddou, J. Mirza, Drying shrinkage, sulphuric acid and sulphate resistance of high-volume palm oil fuel ash-included alkali-activated mortars, *Sustainability* 14 (2022) 498, <https://doi.org/10.3390/su14010498>.
- [23] N. You, Y. Liu, D. Gu, T. Ozbakkaloglu, J. Pan, Y. Zhang, Rheology, shrinkage and pore structure of alkali-activated slag-fly ash mortar incorporating copper slag as fine aggregate, *Constr. Build. Mater.* 242 (2020), 118029, <https://doi.org/10.1016/j.conbuildmat.2020.118029>.
- [24] F. Collins, J.G. Sanjayan, Effect of pore size distribution on drying shrinkage of alkali-activated slag concrete, *Cem. Concr. Res.* 30 (2000) 1401–1406, [https://doi.org/10.1016/S0008-8846\(00\)00327-6](https://doi.org/10.1016/S0008-8846(00)00327-6).
- [25] S. Dueramae, W. Tangchirapat, P. Chindaprasirt, C. Jaturapitakkul, P. Sukontasukkul, Autogenous and drying shrinkages of mortars and pore structure of pastes made with activated binder of calcium carbide residue and fly ash, *Constr. Build. Mater.* 230 (2020), 116962, <https://doi.org/10.1016/j.conbuildmat.2019.116962>.
- [26] W. Chen, H.J.H. Brouwers, Hydration of mineral shrinkage-compensating admixture for concrete: an experimental and numerical study, *Constr. Build. Mater.* 26 (2012) 670–676, <https://doi.org/10.1016/j.conbuildmat.2011.06.070>.
- [27] M. Hojati, A. Radlinska, Shrinkage and strength development of alkali-activated fly ash-slag binary cements, *Constr. Build. Mater.* 150 (2017) 808–816, <https://doi.org/10.1016/j.conbuildmat.2017.06.040>.
- [28] S. Fang, E.S.S. Lam, B. Li, B. Wu, Effect of alkali contents, moduli and curing time on engineering properties of alkali activated slag, *Constr. Build. Mater.* 249 (2020), 118799, <https://doi.org/10.1016/j.conbuildmat.2020.118799>.
- [29] H. Lahalle, V. Benavent, V. Trincal, T. Wattez, R. Bucher, M. Cyr, Robustness to water and temperature, and activation energies of metakaolin-based geopolymer and alkali-activated slag binders, *Constr. Build. Mater.* 300 (2021), 124066, <https://doi.org/10.1016/j.conbuildmat.2021.124066>.
- [30] V. Zivica, Effects of type and dosage of alkaline activator and temperature on the properties of alkali-activated slag mixtures, *Constr. Build. Mater.* 21 (2007) 1463–1469, <https://doi.org/10.1016/j.conbuildmat.2006.07.002>.
- [31] M. Chi, Effects of dosage of alkali-activated solution and curing conditions on the properties and durability of alkali-activated slag concrete, *Constr. Build. Mater.* 35 (2012) 240–245, <https://doi.org/10.1016/j.conbuildmat.2012.04.005>.
- [32] S.K. Das, S. Shrivastava, Influence of molarity and alkali mixture ratio on ambient temperature cured waste cement concrete based geopolymer mortar, *Constr. Build. Mater.* 301 (2021), 124380, <https://doi.org/10.1016/j.conbuildmat.2021.124380>.
- [33] J. Yang, D. Snoeck, N. De Belie, Z. Sun, Effect of superabsorbent polymers and expansive additives on the shrinkage of alkali-activated slag, *Cem. Concr. Compos.* 123 (2021), 104218, <https://doi.org/10.1016/j.cemconcomp.2021.104218>.
- [34] C. Shi, P. Krivenko, D. Roy, *Alkali-Activated Cement and Concretes*, CRC Press, 2006.
- [35] X. Yuan, W. Chen, Z. Lu, H. Chen, Shrinkage compensation of alkali-activated slag concrete and microstructural analysis, *Constr. Build. Mater.* 66 (2014) 422–428, <https://doi.org/10.1016/j.conbuildmat.2014.05.085>.
- [36] J.J. Chang, W. Yeih, C.C. Hung, Effects of gypsum and phosphoric acid on the properties of sodium silicate-based alkali-activated slag pastes, *Cem. Concr. Compos.* 27 (2005) 85–91, <https://doi.org/10.1016/j.cemconcomp.2003.12.001>.
- [37] Q. An, H. Pan, Q. Zhao, S. Du, D. Wang, Strength development and microstructure of recycled gypsum-soda residue-GGBS based geopolymer, *Constr. Build. Mater.* 331 (2022), 127312, <https://doi.org/10.1016/j.conbuildmat.2022.127312>.
- [38] B. Zhang, H. Zhu, P. Feng, P. Zhang, A review on shrinkage-reducing methods and mechanisms of alkali-activated/geopolymer systems: Effects of chemical additives, *J. Build. Eng.* 49 (2022), 104056, <https://doi.org/10.1016/j.jobe.2022.104056>.
- [39] M. Palacios, F. Puertas, Effect of superplasticizer and shrinkage-reducing admixtures on alkali-activated slag pastes and mortars, *Cem. Concr. Res.* 35 (2005) 1358–1367, <https://doi.org/10.1016/j.cemconres.2004.10.014>.
- [40] M. Palacios, F. Puertas, Effect of shrinkage-reducing admixtures on the properties of alkali-activated slag mortars and pastes, *Cem. Concr. Res.* 37 (2007) 691–702, <https://doi.org/10.1016/j.cemconres.2006.11.021>.
- [41] W. Zhang, H. Lin, M. Xue, S. Wang, J. Ran, F. Su, J. Zhu, Influence of shrinkage reducing admixtures on the performance of cementitious composites: A review, *Constr. Build. Mater.* 325 (2022), 126579, <https://doi.org/10.1016/j.conbuildmat.2022.126579>.
- [42] Z. Jia, Y. Yang, L. Yang, Y. Zhang, Z. Sun, Hydration products, internal relative humidity and drying shrinkage of alkali activated slag mortar with expansion agents, *Constr. Build. Mater.* 158 (2018) 198–207, <https://doi.org/10.1016/j.conbuildmat.2017.09.162>.
- [43] T. Bakharev, J.G. Sanjayan, Y.-B. Cheng, Effect of admixtures on properties of alkali-activated slag concrete, *Cem. Concr. Res.* 30 (2000) 1367–1374, [https://doi.org/10.1016/S0008-8846\(00\)00349-5](https://doi.org/10.1016/S0008-8846(00)00349-5).
- [44] S. Hanjitsuwan, B. Injorhor, T. Phoo-ngernkham, N. Damrongwiriyanupap, L.-Y. Li, P. Sukontasukkul, P. Chindaprasirt, Drying shrinkage, strength and microstructure of alkali-activated high-calcium fly ash using FGD-gypsum and dolomite as expansive additive, *Cem. Concr. Compos.* 114 (2020), 103760, <https://doi.org/10.1016/j.cemconcomp.2020.103760>.
- [45] O.A. Mendoza Reales, P.A. Carisio, T.C. dos Santos, W.C. Pearl, R.D. Toledo Filho, Effect of pozzolanic micro and nanoparticles as secondary fillers in carbon nanotubes/cement composites, *Constr. Build. Mater.* 281 (2021), 122603, <https://doi.org/10.1016/j.conbuildmat.2021.122603>.
- [46] Ç. Yalçinkaya, O. Çopuroğlu, Hydration heat, strength and microstructure characteristics of UHPC containing blast furnace slag, *J. Build. Eng.* 34 (2021), 101915, <https://doi.org/10.1016/j.jobe.2020.101915>.
- [47] G. Zhang, H. Yang, C. Ju, Y. Yang, Novel selection of environment-friendly cementitious materials for winter construction: Alkali-activated slag/Portland cement, *J. Clean. Prod.* 258 (2020), 120592, <https://doi.org/10.1016/j.jclepro.2020.120592>.
- [48] K. Boonserm, V. Sata, K. Pimraksa, P. Chindaprasirt, Improved geopolymerization of bottom ash by incorporating fly ash and using waste gypsum as additive, *Cem. Concr. Compos.* 34 (2012) 819–824, <https://doi.org/10.1016/j.cemconcomp.2012.04.001>.
- [49] Z. Shi, C. Shi, S. Wan, N. Li, Z. Zhang, Effect of alkali dosage and silicate modulus on carbonation of alkali-activated slag mortars, *Cem. Concr. Res.* 113 (2018) 55–64, <https://doi.org/10.1016/j.cemconres.2018.07.005>.
- [50] K.-H. Yang, J.-K. Song, A.F. Ashour, E.-T. Lee, Properties of cementless mortars activated by sodium silicate, *Constr. Build. Mater.* 22 (2008) 1981–1989, <https://doi.org/10.1016/j.conbuildmat.2007.07.003>.
- [51] S. Al-Otaibi, Durability of concrete incorporating GGBS activated by water-glass, *Constr. Build. Mater.* 22 (2008) 2059–2067, <https://doi.org/10.1016/j.conbuildmat.2007.07.023>.
- [52] W. Kunther, S. Ferreira, J. Skibsted, Influence of the Ca/Si ratio on the compressive strength of cementitious calcium-silicate-hydrate binders, *J. Mater. Chem. A* 5 (2017) 17401–17412, <https://doi.org/10.1039/C7TA06104H>.
- [53] O.A. Mohamed, M.M. Mustafa, A review of alkali-activated slag as cement replacement, *KEM* 803 (2019) 262–266, <https://doi.org/10.4028/www.scientific.net/KEM.803.262>.
- [54] C.D. Atiş, C. Bilim, Ö. Çelik, O. Karahan, Influence of activator on the strength and drying shrinkage of alkali-activated slag mortar, *Constr. Build. Mater.* (2009) 548–555, <https://doi.org/10.1016/j.conbuildmat.2007.1>.
- [55] C. Shi, R.L. Day, Some factor affecting early hydration of alkali-salg cements, 26 (1996) 439–447, [https://doi.org/10.1016/S0008-8846\(96\)85031-9](https://doi.org/10.1016/S0008-8846(96)85031-9).
- [56] F. Matakah, T. Salem, M. Shaafaey, P. Soroushian, Drying shrinkage of alkali activated binders cured at room temperature, *Constr. Build. Mater.* 201 (2019) 563–570, <https://doi.org/10.1016/j.conbuildmat.2018.12.223>.
- [57] P. Chindaprasirt, S. Thaitwitcharoen, S. Kaewpirom, U. Rattanasak, Controlling ettringite formation in FBC fly ash geopolymer concrete, *Cem. Concr. Compos.* 41 (2013) 24–28, <https://doi.org/10.1016/j.cemconcomp.2013.04.009>.
- [58] D. Balkeere Kumarappa, S. Peethamparan, M. Ngami, Autogenous shrinkage of alkali activated slag mortars: Basic mechanisms and mitigation methods, *Cem. Concr. Res.* 109 (2018) 1–9, <https://doi.org/10.1016/j.cemconres.2018.04.004>.

- [59] S. Aydın, B. Baradan, Effect of activator type and content on properties of alkali-activated slag mortars, *Compos. Part B: Eng.* 57 (2014) 166–172, <https://doi.org/10.1016/j.compositesb.2013.10.001>.
- [60] C. Cartwright, F. Rajabipour, A. Radlińska, Shrinkage characteristics of alkali-activated slag cements, *J. Mater. Civ. Eng.* 27 (2015), [https://doi.org/10.1061/\(ASCE\)MT.1943-5533.0001058](https://doi.org/10.1061/(ASCE)MT.1943-5533.0001058).
- [61] Y. Kong, Investigation of drying shrinkage of alkali-activated cement paste, *IOP Conf. Ser. Earth Environ. Sci.* 567 (2020), 012035, <https://doi.org/10.1088/1755-1315/567/1/012035>.